Simple model for non-Fermi-liquid behavior induced by antiferromagnetic spin fluctuations

P. Schlottmann
Department of Physics, Florida State University, Tallahassee, Florida 32306
(Received 2 June 1998)

We consider a simple model for itinerant antiferromagnetism consisting of an electron pocket and a hole pocket separated by a wave vector **Q**. The nesting of the Fermi surfaces leads to a spin-density wave instability for repulsive Hubbard coupling and to charge-density waves for an attractive interaction. The order can gradually be suppressed by mismatching the nesting and a quantum critical point is obtained as $T_N \rightarrow 0$. In the disordered phase perturbative corrections are logarithmic in the external frequency or the temperature. We investigate the renormalization-group flow of the model in leading and next-to-leading logarithmic order. The linear-response correlation functions for spin-density and charge-density waves are calculated. The specific-heat γ coefficient and the uniform magnetic-field susceptibility increase on a logarithmic scale when the temperature is lowered. The Wilson ratio is temperature dependent and nonuniversal. The Fermi-liquid picture breaks down at the ordering temperature T_N or at a quantum critical point. Our results are valid in the disordered phase for weak and intermediate coupling, but not in the critical region. The results are discussed in the context of non-Fermi-liquid behavior found in some heavy fermion compounds (the two pockets are then part of the Fermi surface of the heavy electron bands). [S0163-1829(99)01319-3]

I. INTRODUCTION

Recently non-Fermi-liquid behavior has been discovered in several heavy fermion compounds and alloys (for experimental reviews see Refs. 1 and 2). The materials that received most attention are $U_{0.2}Y_{0.8}Pd_3$,[3,4] $UCu_{5-x}Pd_x$ for $x=1$, 1.5,[5–7] and $CeCu_{5.9}Au_{0.1}$.[8,9] These systems show deviations from Landau's Fermi-liquid theory in the specific heat, magnetic susceptibility, and the resistivity, typically as a logarithmic or power-law dependence with the temperature over a large temperature interval. The breakdown of the Fermi liquid can be tuned by alloying (chemical pressure) or hydrostatic pressure. In all cases these systems appear to be close to the onset of antiferromagnetic ordering or spin-glass freezing.

There are numerous theoretical attempts to explain these unusual properties. Three scenarios are usually invoked in this context: (i) The vicinity of a zero-temperature quantum phase transition[4,10–13] caused by frustrated spin bonds due to competitions between the Kondo screening of the magnetic moments of the *f* electrons and the Ruderman-Kittel-Kasuya-Yosida interaction between these magnetic moments. (ii) A disorder induced (by alloying other elements) distribution of Kondo temperatures[7,14] with a sufficiently broad width, so that a logarithmic *T* dependence in the susceptibility and the specific heat appears. (iii) A variant of the quadrupolar Kondo effect[15] in which the interaction of the rare-earth (actinide) internal degrees of freedom with the conduction states is reduced to the overcompensated multichannel Kondo model.[16–18] The two-channel Kondo lattice has recently been studied in the infinite-dimension limit with Monte Carlo methods.[19] A fourth possible scenario, proposed to explain the logarithmic dependences in $CeCu_{6-x}Au_x$,[9] are two-dimensional critical ferromagnetic fluctuations coupling to the conduction electrons.

Here we adopt the point of view of a quantum critical point arising from antiferromagnetic correlations with $T_N = 0$. This hypothesis was first proposed by Andraka and Tsvelik.[4] The original idea was followed by a phenomenological scaling theory[10] and renormalization-group treatments of the quantum critical point,[11,12] yielding a rich phase diagram with several crossovers. More recently the self-consistent renormalization theory of spin fluctuations was applied to these systems.[13]

In this paper we consider a band of heavy electrons having two parabolic pockets, one electronlike and the other holelike, separated by a wave vector **Q**.[20] The wave vector **Q** does not have to be commensurate with the reciprocal lattice. A general repulsive interaction between the electrons induces itinerant antiferromagnetism as a consequence of the nesting of the Fermi surfaces of the two pockets.[21] A nesting mismatch is introduced by varying the chemical potential (or a uniform magnetic field), but the temperature and chemical disorder would lead to similar results (due to a smearing of the Fermi surface). With increasing mismatch the Néel temperature is reduced and the long-range order can be suppressed. A quantum critical point is obtained as a limiting case when $T_N \rightarrow 0$.

The interaction is the remaining interaction between heavy quasiparticles after the heavy particles have been formed (in the sense of a Fermi liquid). The interaction consists of three scattering amplitudes and is assumed to be weak. The vertex corrections are logarithmic in the external energy parameter (or the temperature) and are summed to leading and next-to-leading logarithmic order using the multiplicative renormalization group. We study the renormalization-group flow, the linear-response functions for antiferromagnetism, charge-density waves and a uniform magnetic field. The low-temperature specific-heat coefficient and the critical fluctuations of the order parameter are also obtained.

Our main results are the following. For a repulsive interaction the system always renormalizes into a strong-coupling fixed point. In the disordered phase the specific heat can be expressed in terms of an effective mass m^* which increases

on a logarithmic scale as the temperature is lowered. The effective mass diverges at the critical point signaling the breakdown of the Fermi liquid. The magnetic susceptibility can be expressed in terms of the effective mass and a second Fermi-liquid parameter. Both lead to a divergence on a logarithmic scale of the susceptibility when the critical point is approached. The results are valid in the disordered phase in the weak- and intermediate-coupling regime, but not in the strong-coupling or critical region where the perturbative renormalization breaks down. Power laws rather than a logarithmic dependence are expected in the critical region. The results hold for finite T_N, for a quantum critical point ($T_N=0$) or if the order is completely suppressed.

There are several previous applications of the renormalization group to fermionic systems in two and three dimensions. Within Hertz approach[22] the fermionic degrees of freedom are integrated out and an effective bosonic field theory is obtained. Renormalization-group equations for the flow close to the critical point are then derived. This approach, which has been reexamined by Millis[11] in the context of itinerant fermion systems, considers the critical fluctuations about a quantum phase transition. Popov,[23] on the other hand, considered the functional integral method for boson and fermion systems. The variables are divided into ''fast'' and ''slow'' ones and by eliminating the fast ones a renormalized field theory is obtained. This approach has been applied to several phenomena such as superfluidity, superconductivity, and plasmas (Coulomb gas). A systematic and thorough diagrammatic analysis can be found in Shankar's review.[24] The approach here is to integrate out those intermediate states which have an energy (momentum) in a small interval at the ultraviolet cutoff (fast variables). This again leads to an effective action and a fixed-point analysis is made for spherical, nonspherical, and nested Fermi surfaces. A perturbative renormalization-group approach for Fermi liquids was also developed by Hewson.[25] Schulz[26] used the multiplicative renormalization to study the two-dimensional Hubbard model with small deviations from half filling. Multiplicative renormalization is also the method used in this paper. On the one hand, it has the disadvantage that Feynman diagrams have actually to be calculated, while on the other hand, it has the advantage that it provides the resummation of certain classes of diagrams. All the above approaches have in common that the results for a dimension higher than one are very different from those for Luttinger liquids (one dimension).

The rest of the paper is organized as follows. In Sec. II we introduce the model with the three interactions, one small momentum transfer coupling and two with momentum transfer $\mathbf{Q}$ for spin-flip and no spin-flip, respectively. In Sec. III we apply a mean-field factorization for itinerant antiferromagnetism and charge-density waves to the model and obtain the basic conditions for such instabilities. In Sec. IV we study the renormalization-group flow of the model within the leading logarithmic approximation. This investigation is extended in Sec. V to the next-to-leading logarithmic approximation. For repulsive coupling the flow diagram is not changed dramatically by increasing the order of the renormalization. In Sec. VI the correlation functions for the linear response to spin-density and charge-density waves are calculated, as well as the low-temperature specific heat and the magnetic susceptibility to a uniform field. We also briefly address the consequences of a finite stable strong coupling fixed point on the properties of the system. At this point the connection with critical phenomena, in particular a quantum critical point, is made. The critical fluctuations of the order parameter in the normal phase are discussed in Sec. VII. Concluding remarks follow in Sec. VIII.

II. MODEL

The model under consideration consists of one electron and one hole pocket separated by a wave vector $\mathbf{Q}$. Both pockets are assumed to be isotropic with effective masses m_e and m_h, respectively:

$$H_0=\sum_{\mathbf{k}\sigma}\epsilon_e(\mathbf{k})c^\dagger_{\mathbf{k}\sigma}c_{\mathbf{k}\sigma}+\sum_{\mathbf{k}\sigma}\epsilon_h(\mathbf{k}+\mathbf{Q})c^\dagger_{\mathbf{k}+\mathbf{Q}\sigma}c_{\mathbf{k}+\mathbf{Q}\sigma},$$

$$\epsilon_e(\mathbf{k})=\mathbf{k}^2/2m_e,\quad \epsilon_h(\mathbf{k}+\mathbf{Q})=E_0-(\mathbf{k}+\mathbf{Q})^2/2m_h. \quad (1)$$

Here E_0 is the energy difference between the bottom of the electron band and the top of the hole band. The chemical potential μ partially fills both bands, i.e., $0<\mu<E_0$.

The electrons interact with each other via a repulsive potential of the form

$$H_1=\sum_{\mathbf{k}\mathbf{k}'\mathbf{q}\sigma\sigma'}V(\mathbf{q})c^\dagger_{\mathbf{k}\sigma}c_{\mathbf{k}+\mathbf{q}\sigma}c^\dagger_{\mathbf{k}'+\mathbf{q}\sigma'}c_{\mathbf{k}'\sigma'}, \quad (2)$$

where the sum over momenta is over the entire Brillouin zone. We are interested in the states of the two above-mentioned pockets, which we denote with $c^\dagger_{1\mathbf{k}\sigma}$ for the electron pocket and with $c^\dagger_{2\mathbf{k}\sigma}$ for the hole pocket. Here now $\mathbf{k}\approx 0$ refers to the center of the pockets and $|\mathbf{k}|$ is assumed to be small compared to the dimension of the Brillouin zone. The interactions in Hamiltonian (2) can then be separated into interactions among electrons within the same pocket and interactions between the pockets. The former are of the type

$$H_W=W_1\sum_{\mathbf{k}\mathbf{k}'\mathbf{q}\sigma\sigma'}c^\dagger_{1\mathbf{k}\sigma}c_{1\mathbf{k}+\mathbf{q}\sigma}c^\dagger_{1\mathbf{k}'+\mathbf{q}\sigma'}c_{1\mathbf{k}'\sigma'}$$
$$+W_2\sum_{\mathbf{k}\mathbf{k}'\mathbf{q}\sigma\sigma'}c^\dagger_{2\mathbf{k}\sigma}c_{2\mathbf{k}+\mathbf{q}\sigma}c^\dagger_{2\mathbf{k}'+\mathbf{q}\sigma'}c_{2\mathbf{k}'\sigma'}, \quad (3)$$

while the interaction between the two pockets is of the general form

$$H_{12}=V\sum_{\mathbf{k}\mathbf{k}'\mathbf{q}\sigma\sigma'}c^\dagger_{1\mathbf{k}+\mathbf{q}\sigma}c_{1\mathbf{k}\sigma}c^\dagger_{2\mathbf{k}'-\mathbf{q}\sigma'}c_{2\mathbf{k}'\sigma'}$$
$$+U_\parallel\sum_{\mathbf{k}\mathbf{k}'\mathbf{q}\sigma}c^\dagger_{1\mathbf{k}'+\mathbf{q}\sigma}c^\dagger_{2\mathbf{k}-\mathbf{q}\sigma}c_{1\mathbf{k}\sigma}c_{2\mathbf{k}'\sigma}$$
$$+U_\perp\sum_{\mathbf{k}\mathbf{k}'\mathbf{q}\sigma}c^\dagger_{1\mathbf{k}'+\mathbf{q}\sigma}c^\dagger_{2\mathbf{k}-\mathbf{q}-\sigma}c_{1\mathbf{k}-\sigma}c_{2\mathbf{k}'\sigma}. \quad (4)$$

Here V represents the interaction strength for small momentum transfer between the pockets, while $U_\parallel$ and $U_\perp$ correspond to a momentum transfer of $\mathbf{Q}$ without and with spin flip, respectively. There is no need to distinguish between $V_\parallel$ and $V_\perp$, since the additional amplitude can be absorbed into the present form by rearranging the operators. This notation

is essentially the same as for Luttinger liquids,[27,28] although as seen below the physics of this three-dimensional model is very different from a Luttinger liquid. The limit of the Hubbard model (on-site repulsion for electrons with opposite spin) is obtained by choosing $W_1=W_2=V=U_\parallel=U_\perp=U$. The kinetic energy in this notation is

$$H_0=\sum_{l=1,2\,\mathbf{k}\sigma}\epsilon_l(\mathbf{k})c^\dagger_{l\mathbf{k}\sigma}c_{l\mathbf{k}\sigma}, \tag{5}$$

where $\epsilon_1(\mathbf{k})=\epsilon_e(\mathbf{k})$ and $\epsilon_2(\mathbf{k})=\epsilon_h(\mathbf{k})$.

The model, Eqs. (4) and (5), for repulsive interaction leads to itinerant antiferromagnetism with wave vector $\mathbf{Q}$, as a consequence of the nesting of the two Fermi surfaces. This model is similar to that frequently invoked to describe the antiferromagnetism of Cr. In the present context the bands correspond to heavy electrons and holes.

III. MEAN-FIELD APPROXIMATION

In this section we show the existence of antiferromagnetic long-range order for repulsive interaction and charge-density wave order for attractive interaction in the mean-field approximation. The long-range order arises from the nesting of the Fermi surfaces of the two pockets. Hence the interaction leading to the instabilities is contained in H_{12}. In this section we consider the Hamiltonian $H=H_0+H_{12}$ and neglect H_W.

The order parameter for spin- and charge-density wave long-range order is[29]

$$b_\sigma=\sum_{\mathbf{k}}\langle c^\dagger_{2\mathbf{k}\sigma}c_{1\mathbf{k}\sigma}\rangle=\sum_{\mathbf{k}}\langle c^\dagger_{1\mathbf{k}\sigma}c_{2\mathbf{k}\sigma}\rangle. \tag{6}$$

The two pockets contribute to the number of electrons with spin σ at site $\mathbf{R}$ with

$$n_\sigma(\mathbf{R})=\sum_{l\mathbf{k}}\langle c^\dagger_{l\mathbf{k}\sigma}c_{l\mathbf{k}\sigma}\rangle+2\cos(\mathbf{Q}\cdot\mathbf{R})b_\sigma. \tag{7}$$

Hence antiferromagnetic order is obtained when $b_\sigma=-b_{-\sigma}$ and a charge-density wave occurs for $b_\sigma=b_{-\sigma}$.

Factorizing the interaction Hamiltonian H_{12} in terms of b_σ we have

$$H^{MF}_{12}=\sum_{\mathbf{k}\sigma}\Delta_\sigma[c^\dagger_{1\mathbf{k}\sigma}c_{2\mathbf{k}\sigma}+\text{H.c.}]-\sum_\sigma\Delta_\sigma b_\sigma,$$

$$\Delta_\sigma=-Vb_\sigma+U_\parallel b_\sigma+U_\perp b_{-\sigma}, \tag{8}$$

and the off-diagonal one-electron Green's function becomes

$$\langle\langle c_{1\mathbf{k}\sigma};c^\dagger_{2\mathbf{k}\sigma}\rangle\rangle_z=\frac{\Delta_\sigma}{[z-\epsilon_1(\mathbf{k})][z-\epsilon_2(\mathbf{k})]-\Delta^2_\sigma}. \tag{9}$$

For simplicity we assume a constant density of states for electron and hole states. The self-consistency equation for the order parameter is then

$$b_\sigma=\Delta_\sigma\rho_F\int d\epsilon\frac{f(\omega_+)-f(\omega_-)}{\sqrt{(\epsilon_1-\epsilon_2)^2+4\Delta^2_\sigma}}, \tag{10}$$

where

$$\omega_\pm=\frac{1}{2}(\epsilon_1+\epsilon_2)\pm\frac{1}{2}\sqrt{(\epsilon_1-\epsilon_2)^2+4\Delta^2_\sigma}, \tag{11}$$

$\epsilon_1=(m/m_1)\epsilon$ and $\epsilon_2=E_0-(m/m_2)\epsilon$. Here m is the mass of free electrons and ρ_F the density of states for free electrons.

For $T=0$ Eq. (10) can be reduced to

$$b_\sigma=\frac{\gamma}{2}\int_0^{2\epsilon_d}d\epsilon\frac{\theta(\mu-\omega_+)-\theta(\mu-\omega_-)}{\sqrt{(\epsilon-\epsilon_d)^2+\gamma^2}}, \tag{12}$$

where

$$\gamma=2\frac{\Delta_\sigma\rho_F}{\dfrac{m}{m_1}+\dfrac{m}{m_2}},\qquad \epsilon_d=\frac{E_0}{\dfrac{m}{m_1}+\dfrac{m}{m_2}}, \tag{13}$$

and θ is the step function. Here ϵ_d is the energy at which the states of the two pockets have the same energy, i.e., $\epsilon_1=\epsilon_2$. The integral in Eq. (12) yields[29]

$$b_\sigma=\frac{\gamma}{2}\{\operatorname{arcsinh}(X_+/|\gamma|)+\operatorname{arcsinh}(X_-/|\gamma|)\}-\gamma\operatorname{arcsinh}(\epsilon_d/|\gamma|), \tag{14}$$

where $X_+=\epsilon_+-\epsilon_d$ if $|\mu-(m/m_1)\epsilon_d|>\gamma$ and 0 otherwise, and $X_-=\epsilon_d-\epsilon_-$ if $|\mu-(m/m_1)\epsilon_d|>\gamma$ and 0 otherwise. Here $\epsilon_\pm$ correspond to the Fermi surface, i.e., to the two solutions of $\mu=\omega_-(\epsilon)$ if μ lies below the gap or to the two solutions of $\mu=\omega_+(\epsilon)$ if the upper band is intersected by the Fermi energy.

Assume first the Fermi level lies in the gap; then $X_\pm=0$ and for $|\gamma|\ll\epsilon_d$ we have

$$\left(\frac{m}{m_1}+\frac{m}{m_2}\right)b_\sigma=-2\Delta_\sigma\rho_F\ln(\epsilon_d/|\gamma|). \tag{15}$$

This equation only has a solution for antiferromagnetic order if $(V+U_\perp-U_\parallel)>0$ and a charge-density wave solution for $(V-U_\perp-U_\parallel)>0$. If both inequalities are satisfied, the order associated with the larger interaction parameter has the lower ground-state energy and prevails. In the limit of a Hubbard interaction $V=U_\parallel=U_\perp=U$ the system is an itinerant antiferromagnet if $U>0$ and exhibits a charge-density wave if $U<0$. The critical (Néel) temperature is proportional to the gap 2γ and is given by

$$T_c=\epsilon_d\exp\left[-\left(\frac{m}{m_1}+\frac{m}{m_2}\right)\frac{1}{2U\rho_F}\right]. \tag{16}$$

If the Fermi level intersects one of the quasiparticle bands, the terms with $X_\pm$ in Eq. (14) also contribute, reducing the effect of the logarithm in Eq. (15) and hence lowering the critical temperature. The criteria for the formation of antiferromagnetism and charge-density waves remains unchanged. By varying μ the critical temperature can be reduced to zero. The condition on μ for a quantum critical point is

$$\frac{m}{m_1}+\frac{m}{m_2}=(V\pm U_\perp-U_\parallel)\rho_F\times\ln\left(\frac{\epsilon_d^2}{(\epsilon_+-\epsilon_d)(\epsilon_d-\epsilon_-)}\right). \tag{17}$$

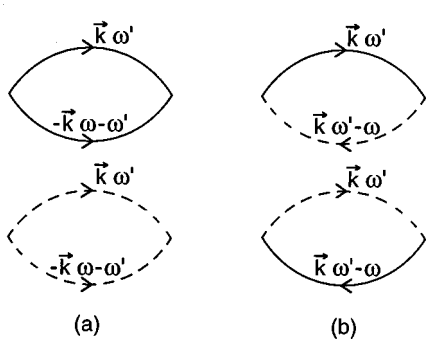

FIG. 1. Diagrams yielding a logarithmic dependence on the energy. (a) Cooper channel (parallel lines) with both particles in the same pockets and (b) zero-sound diagram (antiparallel lines) with one particle in each pocket. The solid lines refer to the electron pocket and the dashed lines to the hole pocket.

The $\pm$ sign refers to the antiferromagnetic and charge-density wave instability, respectively. Note that ϵ_+ and ϵ_- depend on μ. Close to the quantum critical point $|\epsilon_\pm - \epsilon_d|$ can be approximated by $|\mu-(m/m_1)\epsilon_d|$. This parameter is the mismatch in the nesting of the Fermi surfaces, which has the same effect as the smearing of the Fermi surface due to a temperature or a finite mean-free path due to disorder. Below we keep the chemical potential as the mismatch parameter, with the understanding that it can be replaced by a finite T or disorder.

The results depend on the ratio of the effective masses m_1 and m_2, but this dependence is not essential. Below we consider $m_1=m_2=m$ and measure μ from ϵ_d, which simplifies the calculation.

IV. RENORMALIZATION TO LEADING LOGARITHMIC ORDER

As seen from Eq. (15) the antiferromagnetic and charge-density wave instabilities arise from the logarithmic dependence consequence of the integration over the off-diagonal Green's function, Eq. (9). In this section we first investigate which diagrams contribute logarithmically to the interaction vertex and then we study the leading logarithmic renormalization of the model.

The first-order corrections to the vertex are given by the ''bubble'' diagrams. Although the physics of this three-dimensional model is different from a Luttinger liquid, it is useful to adopt the notation and terminology of one-dimensional conductors.[27,28] To first order the bubbles can be classified into the zero-sound and Cooper channels, consisting of antiparallel and parallel propagator lines (see Fig. 1). The propagators correspond either to electrons (solid lines) or to holes (dashed lines). As usual for one-dimensional systems we consider only one external energy variable ω and project all others onto the Fermi level, whenever this is allowed. This is generally not valid in three dimensions, but it is for heavy fermions where the energy dependence is much more important than the dependence on the momentum. The energy ω is assumed to be small compared to the cutoff energy ϵ_d, and the density of states for electrons and holes is assumed to be a constant, ρ_F.

The zero-sound bubble (antiparallel lines) involving only electrons (or only holes) is given by

$$-i\int\frac{d^3k'}{(2\pi)^3}\int\frac{d\omega'}{2\pi}G_1(\mathbf{k}',\omega')G_1(\mathbf{k}'+\mathbf{k},\omega'+\omega). \tag{18}$$

This integral is sensitive to the order in which k and ω tend to zero, but fortunately it is independent of the cutoff and hence not relevant to the renormalization. If $k=0$ its contribution vanishes, while if $\omega=0$ the $k\to 0$ limit yields ρ_F. The corresponding Cooper channel diagram [parallel lines, see Fig. 1(a)] has a logarithmic dependence:

$$-i\int\frac{d^3k}{(2\pi)^3}\int\frac{d\omega'}{2\pi}G_1(\mathbf{k},\omega')G_1(-\mathbf{k},-\omega'+\omega) = -\rho_F\ln[(|\omega|+2|\mu|)/(2\epsilon_d)]. \tag{19}$$

Similarly, the zero-sound bubble with one electron and one hole line [see Fig. 1(b)] is logarithmic, namely,

$$-i\int\frac{d^3k}{(2\pi)^3}\int\frac{d\omega'}{2\pi}G_1(\mathbf{k},\omega')G_2(\mathbf{k},\omega'-\omega) = \rho_F\ln[(|\omega|+2|\mu|)/(2\epsilon_d)], \tag{20}$$

while for the Cooper channel loop we have

$$-i\int\frac{d^3k'}{(2\pi)^3}\int\frac{d\omega'}{2\pi}G_1(\mathbf{k}',\omega')G_2(-\mathbf{k}'-\mathbf{k},-\omega'+\omega). \tag{21}$$

This diagram is formally similar to Eq. (18), but there is a significant difference: As a consequence of the mismatch between the Fermi surfaces the limit $\omega\to 0$ and $k\to 0$ is not sensitive to the order of the limits and yields $-\rho_F$. This contribution has no cutoff dependence and is irrelevant to the renormalization.

A Luttinger liquid has forward and backward moving electrons, the backward moving particles playing a similar role as the holes in the present model.[28] For a one-dimensional gas of electrons all of the four bubbles are logarithmically divergent. The cancellations among the diagrams leads to the renormalization of the group velocities and hence to the well-known charge and spin separation. This is not the case for the present model, since it is three-dimensional.

Within the leading logarithmic approximation we only need to sum up consistently the divergent diagrams. For the interaction $W_1=W_2=W$ this corresponds to a summation over the ladder diagrams of the type (19). Denoting $\xi=\ln[2\epsilon_d/(|\omega|+2|\mu|)]$ the renormalized interaction $\tilde{W}$ becomes

$$\tilde{W}=\frac{W\rho_F}{1+W\rho_F\xi}; \tag{22}$$

hence the interaction strength $\tilde{W}$ is reduced with respect to $W\rho_F$ for repulsive W, but enhanced for attractive W. This is not surprising, since the vertex (22) exhibits the BCS-pole and Cooper-pair bound states are only formed for $W<0$. This interaction decouples from the interactions between electrons and holes (V, $U_\parallel$, and $U_\perp$), and, since we are

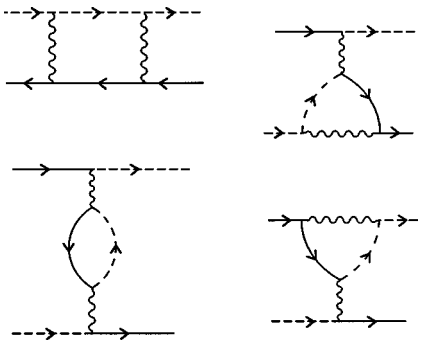

FIG. 2. The four first-order diagrams contributing logarithmically to the renormalization of the vertex to leading order. The wavy line represents one of the three interactions, V, $U_\parallel$, and $U_\perp$. All diagrams are of the zero-sound type.

interested in repulsive interactions, it will be neglected throughout the rest of the paper.

The four logarithmic diagrams contributing to the renormalization of the interactions of Eq. (4) are shown in Fig. 2. They lead to the following renormalization-group equations:

$$\frac{d\tilde{V}}{d\xi}=\tilde{V}^2,$$

$$\frac{d\tilde{U}_\parallel}{d\xi}=-\tilde{U}_\parallel^2-\tilde{U}_\perp^2+2\tilde{U}_\parallel\tilde{V},$$

$$\frac{d\tilde{U}_\perp}{d\xi}=-2\tilde{U}_\perp(\tilde{U}_\parallel-\tilde{V}). \tag{23}$$

The integration of these equations is straightforward:

$$\tilde{V}=\frac{V\rho_F}{1-V\rho_F\xi},$$

$$\tilde{U}_\parallel\pm\tilde{U}_\perp-\tilde{V}=\frac{(U_\parallel\pm U_\perp-V)\rho_F}{1+(U_\parallel\pm U_\perp-V)\rho_F\xi}. \tag{24}$$

The system is then strongly coupled if $V>0$ and/or $(U_\parallel\pm U_\perp-V)<0$, because at least one of the vertices will be divergent. In the Hubbard limit $U_\parallel=U_\perp=V$ the model is always strongly coupled unless $U=0$.

Of interest is also the renormalization-group flow diagram arising from Eq. (23). For simplicity we assume spin-rotational invariance, i.e., $U_\parallel=U_\perp=U$. There are then two independent couplings, namely V, the small momentum-transfer parameter, and U, the large momentum transfer interaction. The flow diagram is shown in Fig. 3. As argued above, the fixed points correspond either to strong coupling (the flow goes to infinity) or weak coupling (the flow goes into the origin). We stress the fact that for $V>0$ or $V-2U>0$ the system is always strongly coupled.

V. RENORMALIZATION TO NEXT-TO-LEADING LOGARITHMIC ORDER

It is important to analyze if the renormalization-group flow changes dramatically if next-to-leading logarithmic order diagrams are included, although once the system flows

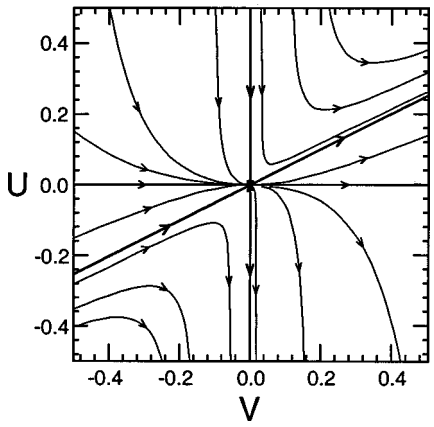

FIG. 3. Leading logarithmic order renormalization-group flow for the vertex amplitudes V and $U_\parallel=U_\perp=U$. There are two stable fixed points, one weak-coupling fixed point $V=U=0$, and the strong-coupling fixed point (the couplings flow to infinity).

toward a strong-coupling fixed point it cannot be brought back by higher-order renormalization. In other words, the second-order corrections to the vertex functions have to be computed. Three types of contributions arise: (i) terms proportional to ξ^2, (ii) terms proportional to ξ, and (iii) cutoff independent terms. The latter are neglected in the renormalization. The terms of type (i) are part of the leading-order diagrams and are obtained by inserting zero-sound diagrams into zero-sound diagrams. They are already generated by the leading-order renormalization-group equations, Eq. (23).

There are three kinds of corrections proportional to ξ [class (ii)] contributing to the vertex for the interaction between the electron pocket and the hole pocket. Two kinds are of the type of parquet diagrams and the third kind of vertex contribution is known as the ''third channel'' in diagrammatic approaches to the Kondo problem and to Luttinger liquids.[27,28,30] Although the classification of diagrams is the same as in one dimension, the outcome is very different. The parquet diagrams correspond to inserting a first-order zero-sound vertex correction into a Cooper channel bubble and vice versa, inserting a first-order Cooper channel vertex correction into the zero-sound bubble. The evaluation of these diagrams involves an eightfold integration, but we are actually only interested in the cutoff dependence in the limit where all external variables tend to zero. In order to evaluate the contributions proportional to ξ we assume a nesting mismatch and we approximate the vertex insertion by assuming that it depends only on one external variable (this approximation is known to be exact in one dimension).

The ''third channel'' contributions are related to the self-energy via the Ward identities for the conservation of charge in each pocket and the total spin. Their cutoff dependence can be obtained by differentiating self-energy diagrams (shown in Fig. 4) with respect to the external energy. The differentiation is equivalent to an insertion of a bare vertex which transforms a self-energy diagram into a vertex diagram.

We limit ourselves to summarize the final perturbative result to next-to-leading order for the vertices Γ:

$$\delta(V\Gamma_V)=[4V^3+6VU_\perp^2-4U_\parallel U_\perp^2]\rho_F^2\xi + [2V^3-2V^2U_\parallel+V(U_\parallel^2+U_\perp^2)-U_\parallel U_\perp^2]\rho_F^2\xi,$$

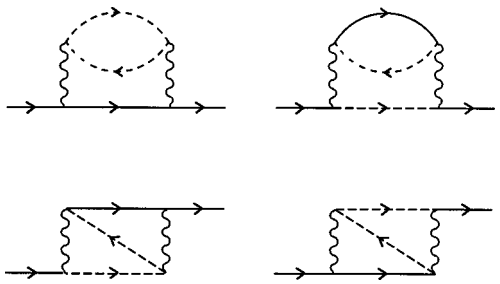

FIG. 4. The four lowest-order logarithmic self-energy diagrams.

$$\delta(U_\parallel\Gamma_\parallel)=[6V^2U_\parallel+V(U_\parallel^2-U_\perp^2)-3V(U_\parallel^2+U_\perp^2)+U_\parallel U_\perp^2]\rho_F^2\xi+[2V^2U_\parallel-2VU_\parallel^2+U_\parallel(U_\parallel^2-U_\perp^2)]\rho_F^2\xi,$$

$$\delta(U_\perp\Gamma_\perp)=[6V^2U_\perp-6VU_\parallel U_\perp+U_\parallel^2U_\perp]\rho_F^2\xi+[2V^2U_\perp-2VU_\parallel U_\perp]\rho_F^2\xi, \quad (25)$$

where the first brackets correspond to the ''parquet'' corrections and the second brackets to the ''third channel.''

In order to obtain the invariant couplings $\tilde{V}$, $\tilde{U}_\parallel$, and $\tilde{U}_\perp$ we need in addition the self-energy corrections. The second-order self-energy diagrams are shown in Fig. 4. They involve integrations over two nested energy and momentum loops. The three dimensionality of the phase space makes the evaluation of these integrals rather difficult. Since we are only interested in the logarithmic dependence on the cutoff, we may place the external momentum at the Fermi surface of the corresponding pocket and average over the Fermi sphere (all possible directions). Furthermore, one of the propagators carries an energy $\epsilon(\mathbf{k}+\mathbf{q})$, i.e.,

$$\epsilon(\mathbf{k}+\mathbf{q})=\frac{k^2}{2m}+\frac{q^2}{2m}+\frac{1}{m}\mathbf{k}\cdot\mathbf{q}; \quad (26)$$

averaging the propagator $G(\mathbf{k}+\mathbf{q},\omega)$ over the relative orientation of the vectors $\mathbf{k}$ and $\mathbf{q}$ we obtain that the logarithmic cutoff dependence is recovered if we replace $\epsilon(\mathbf{k}+\mathbf{q})\approx\epsilon(\mathbf{k})+\epsilon(\mathbf{q})$, i.e., neglecting the scalar product $\mathbf{k}\cdot\mathbf{q}$. The same approximation has been used for the evaluation of the ''third channel'' vertex diagrams. Keeping only the external energy variable (valid only for heavy fermions, where the $\mathbf{k}$ dependence can be neglected) the self-energy corrections are then

$$\Sigma(\omega)=-\frac{1}{2}\omega[U_\parallel^2+U_\perp^2-2U_\parallel V+2V^2]\rho_F^2\xi. \quad (27)$$

The self-energy is the same for the electron pocket as for the hole pocket. Perturbatively to next leading order the multiplicative renormalization of a propagator is then given by

$$d(\omega)=1-\frac{1}{2}[U_\parallel^2+U_\perp^2-2U_\parallel V+2V^2]\rho_F^2\xi. \quad (28)$$

The ''invariant couplings'' of the model are obtained from the product of a vertex times two Green's functions, i.e., $\Gamma(\omega)d(\omega)^2$. This product gives rise to several Ward identity cancellations between the vertex parts [third channel, given by the second brackets in Eq. (25)] and the self-energy, Eq. (28). The resulting renormalization-group equations are

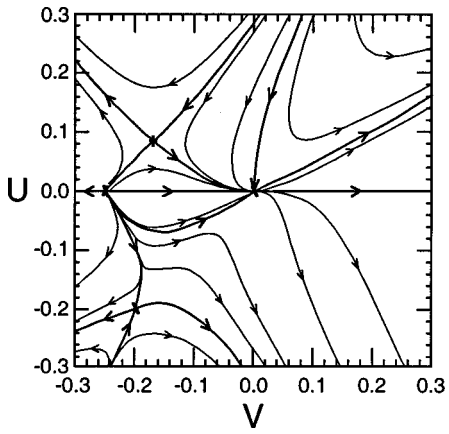

FIG. 5. Next-to-leading logarithmic order renormalization-group flow for the invariant couplings $\tilde{V}$ and $\tilde{U}_\parallel=\tilde{U}_\perp=\tilde{U}$. In addition to the two stable fixed points, one weak coupling fixed point ($V=U=0$) and the strong-coupling fixed point (the couplings flow to infinity), there are two unstable fixed points in the attractive coupling region of the diagram.

$$\frac{d\tilde{V}}{d\xi}=\tilde{V}^2+[4\tilde{V}^3+6\tilde{V}\tilde{U}_\perp^2-5\tilde{U}_\parallel\tilde{U}_\perp^2],$$

$$\frac{d\tilde{U}_\parallel}{d\xi}=-\tilde{U}_\parallel^2-\tilde{U}_\perp^2+2\tilde{U}_\parallel\tilde{V}+[12\tilde{V}^2\tilde{U}_\parallel-8\tilde{V}\tilde{U}_\perp^2-4\tilde{V}\tilde{U}_\parallel^2],$$

$$\frac{d\tilde{U}_\perp}{d\xi}=-2\tilde{U}_\perp(\tilde{U}_\parallel-\tilde{V})+[12\tilde{V}^2-12\tilde{V}\tilde{U}_\parallel+\tilde{U}_\parallel^2-\tilde{U}_\perp^2]\tilde{U}_\perp. \quad (29)$$

The last two equations become identical in the limit $\tilde{U}_\parallel=\tilde{U}_\perp$. Hence the renormalization-group equations preserve the spin rotational invariance. On the other hand, the Hubbard limit is not a solution of these equations, i.e., starting with $V=U_\parallel=U_\perp$ the system renormalizes away so that in general $\tilde{V}\neq\tilde{U}$.

The renormalization-group flow diagram for $\tilde{U}_\parallel=\tilde{U}_\perp=\tilde{U}$ is shown in Fig. 5. In this limit the Eqs. (29) reduce to

$$\frac{d\tilde{V}}{d\xi}=\tilde{V}^2+4\tilde{V}^3+6\tilde{V}\tilde{U}^2-5\tilde{U}^2,$$

$$\frac{d\tilde{U}}{d\xi}=-2(\tilde{U}-\tilde{V})\tilde{U}(1+6\tilde{V}). \quad (30)$$

The fixed points are given by the zeros of the right-hand side of Eq. (30). Besides the stable weak-coupling fixed point (origin) and the stable strong-coupling fixed point (at infinity), there are two unstable fixed points at

$$\tilde{V}^*=-1/6, \quad \tilde{U}^*=0.0814,$$

$$\tilde{V}^*=-0.2, \quad \tilde{U}^*=-0.2. \quad (31)$$

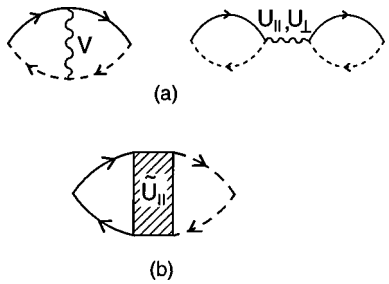

FIG. 6. (a) Leading logarithmic order diagrams for the spin-density and charge-density wave response function. (b) Vertex insertion for the uniform magnetic-field susceptibility.

The flow is not substantially modified by the next-to-leading contributions for repulsive coupling, i.e., within the first quadrant. There is no new fixed point and the system still renormalizes toward the strong-coupling fixed point. There are, however, considerable changes in the attractive region. It is not clear from this calculation if the unstable fixed points and the concommitant changes in the flow diagram, consequence of the next-to-leading order renormalization, are physically meaningful (i.e., are caused by a new instability) or would be changed again within a higher-order renormalization.

In summary, from these results no physical changes are expected in the region (the first, fourth, and lower part of the third quadrants) where itinerant antiferromagnetism and charge-density waves are stable. Hence for the rest of the paper we restrict ourselves to calculate response functions within the leading logarithmic approximation, which already yields qualitatively correct results.

VI. CORRELATION FUNCTIONS AND SPECIFIC HEAT

In this section we first calculate the linear response of the system to itinerant antiferromagnetism and to charge-density waves. Then we consider the low-temperature specific heat and the response to a uniform magnetic field.

A. Antiferromagnetic response

The linear response of the system to a staggered field of periodicity $\mathbf{Q}$ is given by

$$\chi_S(\mathbf{Q},\omega) = -i\int dt \langle T\{O(\mathbf{Q},t)O^{\dagger}(\mathbf{Q},0)\}\rangle, \tag{32}$$

where

$$O(\mathbf{Q}) = \sum_{\mathbf{k}} [c^{\dagger}_{1\mathbf{k}\uparrow}c_{2\mathbf{k}\uparrow} - c^{\dagger}_{1\mathbf{k}\downarrow}c_{2\mathbf{k}\downarrow}]; \tag{33}$$

$\langle \cdots \rangle$ denotes expectation value and T stands for time-ordered product.

The perturbation expansion of this correlation function in terms of V, $U_{\parallel}$, and $U_{\perp}$ in leading logarithmic approximation is [the first-order diagrams are displayed in Fig. 6(a)]

$$\chi_S(\mathbf{Q},\omega) = -2\rho_F\xi[1+(V-U_{\parallel}+U_{\perp})\rho_F\xi+\cdots]. \tag{34}$$

Due to the fact that the zeroth-order term has a logarithmic dependence, this susceptibility does not satisfy the criterion of multiplicative renormalization.[31] This is analogous to susceptibility of the x-ray threshold problem and to the corresponding response function for a Luttinger liquid. An auxiliary quantitity is introduced, $\bar{\chi}_S(\omega) = -(2\rho_F)^{-1}(\partial\chi_S/\partial\xi)$, which is normalized to unity at the cutoff energy. This quantity satisfies the scaling hypothesis and gives rise to the following renormalization-group equation:

$$\frac{\partial \ln \bar{\chi}_S}{\partial \xi} = 2(\tilde{V}-\tilde{U}_{\parallel}+\tilde{U}_{\perp}). \tag{35}$$

The integration of this equation yields

$$\bar{\chi}_S = \frac{1}{[1-(V-U_{\parallel}+U_{\perp})\rho_F\xi]^2},$$

$$\chi_S = -\frac{2\rho_F\xi}{1-(V-U_{\parallel}+U_{\perp})\rho_F\xi}, \tag{36}$$

which reproduces the perturbation expansion, Eq. (34). The divergence at $\xi = 1/[\rho_F(V-U_{\parallel}+U_{\perp})]$ signals the antiferromagnetic instability at $T_N = 2\epsilon_d \exp\{-1/[\rho_F(V-U_{\parallel}+U_{\perp})]\} - 2|\mu|$. Note that μ represents the mismatch between the two Fermi surfaces and is measured from ϵ_d. This result agrees with the mean-field result of Sec. III. The condition for a quantum critical point is $T_N = 0$, and if $T_N < 0$ the response function is always finite signaling that the system has not developed antiferromagnetic long-range order. We return to this issue in the next section when we discuss the critical fluctuations.

B. Charge-density wave response

The linear response of the system to a charge-density wave is given by a correlation function similar to Eq. (32), but with

$$O(\mathbf{Q}) = \sum_{\mathbf{k}} [c^{\dagger}_{1\mathbf{k}\uparrow}c_{2\mathbf{k}\uparrow} + c^{\dagger}_{1\mathbf{k}\downarrow}c_{2\mathbf{k}\downarrow}]. \tag{37}$$

Again, the perturbation expansion of this susceptibility in leading logarithmic approximation is given by the diagrams shown in Fig. 6(a):

$$\chi_c(\mathbf{Q},\omega) = -2\rho_F\xi[1+(V-U_{\parallel}-U_{\perp})\rho_F\xi+\cdots]. \tag{38}$$

Again, this susceptibility does not satisfy multiplicative renormalization, so that we introduce the auxiliary quantitity, $\bar{\chi}_c(\omega) = -(2\rho_F)^{-1}(\partial\chi_c/\partial\xi)$, which has the correct scaling properties.[31] The renormalization-group equation

$$\frac{\partial \ln \bar{\chi}_c}{\partial \xi} = 2(\tilde{V}-\tilde{U}_{\parallel}-\tilde{U}_{\perp}) \tag{39}$$

is straightforwardly integrated yielding

$$\bar{\chi}_c = \frac{1}{[1-(V-U_{\parallel}-U_{\perp})\rho_F\xi]^2},$$

$$\chi_c = -\frac{2\rho_F\xi}{1-(V-U_{\parallel}-U_{\perp})\rho_F\xi}. \tag{40}$$

The divergence at $\xi = 1/[\rho_F(V-U_{\parallel}-U_{\perp})]$ signals the instability to a charge-density wave at $T_c = 2\epsilon_d \exp\{-1/[\rho_F(V$

$-U_{\parallel}-U_{\perp})]\}-2|\mu|$, where μ again represents the mismatch between the two Fermi surfaces. This result agrees with the mean-field result of Sec. III. For initial conditions corresponding to the Hubbard model, $V=U_{\parallel}=U_{\perp}=U>0$, the model is not unstable to charge-density waves, but will exhibit antiferromagnetism if the mismatch between the Fermi surfaces is not too large.

C. Low-temperature specific heat

At low temperatures the specific heat is proportional to T. The γ coefficient is determined by the derivative of the self-energy with respect to the external energy $i\omega$, i.e.,[32,33]

$$\gamma=\frac{4\pi^2}{3}\rho_F\left[1-\frac{\partial\Sigma(\omega)}{\partial i\omega}\right]_{\omega=0}, \tag{41}$$

where the factor 4 arises from the spin degeneracy and the two bands. Here the external momentum of the self-energy is averaged over the Fermi surface. In the remainder of this section we use the finite temperature formalism, so that $\omega\rightarrow i\omega$ is the analytic continuation of the Matsubara poles.[33] The renormalized quantity $[1-\partial\Sigma/\partial i\omega]$ is just the inverse of $d(\omega)$, Eq. (28), which satisfies the renormalization-group equation (we have neglected the $\mathbf{k}$ dependence of Σ, which is a valid approximation only for heavy fermions)

$$\frac{d\ln d(\omega)}{d\xi}=-\frac{1}{2}[\tilde{U}_{\parallel}^2+\tilde{U}_{\perp}^2-2\tilde{U}_{\parallel}\tilde{V}+2\tilde{V}^2]=\frac{d}{d\xi}\left(\tilde{V}-\frac{1}{2}\tilde{U}_{\parallel}\right), \tag{42}$$

so that

$$\ln d(\omega)=-\frac{1}{4}\frac{(U_{\parallel}+U_{\perp}-V)^2\rho_F^2\xi}{1+(U_{\parallel}+U_{\perp}-V)\rho_F\xi}-\frac{1}{4}\frac{(U_{\parallel}-U_{\perp}-V)^2\rho_F^2\xi}{1+(U_{\parallel}-U_{\perp}-V)\rho_F\xi}-\frac{1}{2}\frac{(V\rho_F)^2\xi}{1-V\rho_F\xi}. \tag{43}$$

The specific-heat coefficient can then be written as

$$\frac{\gamma}{\gamma_0}=\frac{1}{d(T)}=\frac{m^*(T)}{m}, \tag{44}$$

where γ_0 is the value for the noninteracting system and $d(T)$ is expression (43) with $\xi=\ln[\epsilon_d/(T+|\mu|)]$. Hence the specific heat γ coefficient increases as the temperature is lowered on a logarithmic scale. For an interaction of the Hubbard-type $(U>0)$, we obtain

$$\frac{m^*(T)}{m}=\exp\left[\frac{3}{4}\frac{(U\rho_F)^2\xi}{1-U\rho_F\xi}\right] \tag{45}$$

with $m^*(T)$ being the temperature-dependent effective thermal mass. Note that γ diverges at the Néel temperature, but remains finite if the system does not order. At the quantum critical point γ diverges signaling the breakdown of the Fermi-liquid theory.

D. Uniform field susceptibility

The magnetic susceptibility can be calculated either as a response function or through Fermi-liquid relations. The corresponding operator is

$$O_B=\sum_{\mathbf{k}\sigma}\sigma[c_{1\mathbf{k}\sigma}^{\dagger}c_{1\mathbf{k}\sigma}+c_{2\mathbf{k}\sigma}^{\dagger}c_{2\mathbf{k}\sigma}]. \tag{46}$$

Through Fermi-liquid relations the susceptibility is expressed in terms of the field derivative of the self-energy of a particle with spin σ:[32,34,35]

$$\chi_B=\mu_B^2\rho_F\left[1-\frac{1}{2}\sum_{\sigma\sigma'}\sigma\sigma'\frac{\partial\Sigma_{\sigma}(\omega=0)}{\partial B_{\sigma'}}\right], \tag{47}$$

where $B_{\sigma'}$ is the field acting on a propagator of spin σ' and the energy is fixed at the Fermi level. The external momentum in the self-energy is averaged over the Fermi surface. For heavy fermions the momentum dependence can be neglected. For instance, the derivative of the self-energy of an electron of spin σ with respect to the magnetic field carried by a propagator for a particle in the hole pocket with spin σ' is[33,34]

$$\frac{\partial\Sigma_{1\sigma}(\omega=0)}{\partial B_{\sigma'}}=-\rho_F\int\frac{d\omega'}{2\pi}\int d\epsilon'\times\Gamma_{1\sigma,2\sigma'}(0,0;\epsilon',\omega')\times[G_{2\sigma'}(\epsilon',\omega')]^2. \tag{48}$$

Here we replaced the momentum integration by one over ϵ'. The derivative of $\Sigma_{1\sigma}(\omega)$ with respect to $i\omega$ has similar terms, and in addition there is another term. This additional term arises from the discontinuity of the propagator $G_{2\sigma'}(\epsilon',\omega')$ along the real axis, i.e., when the derivative crosses from the upper $i\omega'$ half plane to the lower one, which is proportional to $\delta(\omega')\delta(\epsilon'-\mu)$. Hence, the field derivative of the self-energy is related to the frequency derivative via[34]

$$\sum_{\sigma}\left.\frac{\partial\Sigma_{\sigma}}{\partial i\omega}\right|_{\omega=0}=\sum_{\sigma\sigma'}\sigma\sigma'\frac{\partial\Sigma_{\sigma}(\omega=0)}{\partial B_{\sigma'}}+\sum_{\sigma\sigma'}\sigma\sigma'\rho_F\Gamma_{\sigma\sigma',\sigma'\sigma}(0,0;0,0). \tag{49}$$

This corresponds to the Ward identity for the conservation of the total spin.[34,35] As a consequence of the form of the operator O_B the only possible interaction vertices contributing to Eq. (49) are Γ_W and $\Gamma_{U_{\parallel}}$. Hence the susceptibility is given by

$$\begin{aligned}\chi_B&=\mu_B^2\rho_F\left[1-\frac{\partial\Sigma}{\partial\omega}+\rho_F W\Gamma_W+\rho_F U_{\parallel}\Gamma_{U_{\parallel}}\right]_{\omega=0}\\&=\mu_B^2\rho_F\{[d(T)]^{-1}+[d(T)]^{-2}[\tilde{W}+\tilde{U}_{\parallel}]\}\\&=\mu_B^2\rho_F\frac{m^*(T)}{m}\left[1+\frac{m^*(T)}{m}(\tilde{W}+\tilde{U}_{\parallel})\right].\end{aligned} \tag{50}$$

The first part of the renormalization of χ_B corresponds to self-energy insertions, which give rise to the effective mass. The second part represents the vertex insertion as shown in

Fig. 6(b). Note that $\xi=\ln[\epsilon_d/(T+|\mu|)]$ in the vertices. Here $\tilde{W}$ renormalizes to zero for repulsive interactions and can be neglected. As the critical point is approached, both m^* and $\tilde{U}_\parallel$ diverge, signaling the breakdown of the Fermi liquid.

The Wilson ratio takes a simple form,

$$\frac{\chi_B/\chi_{B0}}{\gamma/\gamma_0}=1+\frac{m^*(T)}{m}\tilde{U}_\parallel, \tag{51}$$

which is nonuniversal and temperature dependent. Note that at the quantum critical point γ, χ_B, and the Wilson ratio all diverge. These expressions are also valid if no long-range order takes place (suppressed antiferromagnet).

E. Finite fixed point

The present approach is perturbative, i.e., valid only as long as the coupling constants are sufficiently small. Otherwise loops to all order have to be included. In other words, with this method we cannot reach into the critical regime. The renormalization-group flow to strong coupling cannot be reversed by higher-order diagrams, but we are unable to decide if the flow ends in a finite fixed point or if this fixed point is at infinity.

In this subsection we briefly speculate on the consequences of a strong-coupling fixed point at a finite coupling, i.e., when the renormalization-group flow merges to a finite point rather than infinity. The critical behavior for the spin-density and charge-density wave correlation functions is then given by the fixed point, i.e., in Eqs. (35) and (39) the right-hand side is given by a constant (the values of $\tilde{V}$, $\tilde{U}_\parallel$, and $\tilde{U}_\perp$ at the fixed point). The integration leads then to a power-law dependence of these correlation functions, $(T-T_N)^{-x}$, with the critical exponents determined by the couplings at the fixed point.

Similarly $d(T)$ follows a power-law rather than a logarithmic dependence, and hence the temperature dependence of the effective mass would be increasing with a power of $T-T_N$ as $T\to T_N$. The same is true for the magnetic response to a uniform field.

Hence there is a crucial difference between a strong coupling fixed at infinity, for which a temperature dependence remains on a logarithmic scale, and a fixed point at finite coupling, where the dependence is logarithmic in the precritical region and gradually crosses over to a power law in the critical region. This latter seems to correspond more to the experimental situation for which $T_N\simeq 0$.

VII. PRECRITICAL FLUCTUATIONS

In this section we briefly consider the energy (or temperature) dependence of the antiferromagnetic order parameter in the precritical region. For simplicity we assume the conditions of the Hubbard interaction. The procedure is similar to the one employed previously to superconducting fluctuations in Luttinger liquids[36] and for the ground state of the Kondo problem.[37] To stress this analogy (the physics is different, but in all cases the variation is on a logarithmic scale) we denote the order parameter here with $\Delta(\xi)$, but for $\xi=0$ it is equal to b_σ defined in Sec. II.

Since the dependence of the correlation functions on the energy is logarithmic, ξ is the natural variable for the order parameter. The integral equation satisfied by $\Delta(\xi)$ is

$$\Delta(\xi)=\int_0^{\xi_0}d\xi'\frac{U\rho_F}{1-U\rho_F\xi'}\Delta(\xi'')\approx\frac{U\rho_F}{1-U\rho_F\xi}\int_\xi^{\xi_0}d\xi'\,\Delta(\xi')+\int_0^{\xi}d\xi'\frac{U\rho_F}{1-U\rho_F\xi'}\Delta(\xi'), \tag{52}$$

where $\xi'=\ln(\epsilon_d/|\omega'|)$, $\xi''=\ln(\epsilon_d/|\omega+\omega'|)$ and ξ_0 is a cutoff of the order of $1/(U\rho_F)$. The second step in Eq. (52) involves the logarithmic approximation. The integral equation is conveniently simplified by differentiation with respect to ξ,

$$\frac{d\Delta}{d\xi}=\left(\frac{U\rho_F}{1-U\rho_F\xi}\right)^2\int_\xi^{\xi_0}d\xi'\,\Delta(\xi'). \tag{53}$$

The solution of this equation is of the form

$$\Delta(\xi)=A(1-U\rho_F\xi)^\alpha, \tag{54}$$

where A is an arbitrary complex constant, α satisfies $\alpha(\alpha+1)+1=0$, and $U\rho_F\xi_0=1$. The two roots for α are complex conjugated, $\alpha_\pm=-1/2\pm i\sqrt{3}/2$. The solution of Eq. (53) requires two integration constants, which can be absorbed into a complex amplitude A', so that

$$\Delta(\xi)=A'\left(\frac{U\rho_F}{1-U\rho_F\xi}\right)^{1/2}. \tag{55}$$

This result does not change (U is replaced by $V+U_\perp-U_\parallel$) if the more general interaction is considered. A similar result is obtained for fluctuations of the charge-density wave order parameter, only that instead of U we have $V-U_\perp-U_\parallel$. The fluctuations of the order parameter diverge at the critical point. The amplitude A' is proportional to the gap, i.e., nonanalytic in the coupling. To derive Eq. (55) we used the vertex function obtained via perturbative renormalization. Hence this expression only includes precritical fluctuations. As the system approaches the fixed point (e.g., a finite coupling fixed point) there will be a crossover to a power-law dependence (critical behavior).

The order parameter enters the free energy as $|\Delta(\xi)|^2$, which has the same ξ dependence as the vertex. These contributions have already been taken into account perturbatively in the previous section and should not be incorporated again (double counting).

The result, Eq. (55), is different from similar approaches for the Kondo problem (Yosida's ansatz for the ground-state wave function[37]) and one dimensional conductors.[36] In the Kondo case the spin dependence of the interaction leads to two different real values for α, which are both needed to get a complete solution. Moreover, in the Kondo problem and for Luttinger liquids there are additional cancellations between the zero-sound and Cooper channels, which are absent in the present case. This interference leads to a smaller exponent (1/4 instead of 1/2) for the superconducting fluctuations in Luttinger liquids.[36]

In Sec. IV, Eq. (24), we obtained three combinations of invariant couplings. Two of them, namely $U_\parallel\pm U_\perp-V$, were

identified with itinerant antiferromagnetism and charge-density waves, respectively. The ordered magnetic moment in this case is parallel to the axis of spin quantization. This leads to the question, what is the order parameter associated with the third invariant coupling V? By inspection of the Hamiltonian we see that the interaction leads to an anomalous coupling of the form $\Sigma_{\mathbf{k}}\langle c^{\dagger}_{1\mathbf{k}\uparrow}c_{2\mathbf{k}\downarrow}\rangle$, which also corresponds to itinerant antiferromagnetism but with ordered magnetic moment in the plane perpendicular to the axis of spin quantization. Note that in the case of spin isotropy ($U_{\parallel}=U_{\perp}$) the two singularities coincide and hence, as expected, the Néel temperature is the same for both cases.

VIII. CONCLUDING REMARKS

We considered a simple model for itinerant antiferromagnetism consisting of a Fermi surface with one electron pocket and a hole pocket separated by a wave vector **Q**. These pockets are assumed to be part of the heavy electron band of a heavy fermion compound. The electrons of both pockets interact with each other via a weak repulsive force, which is the remainder of strong correlations after the heavy particles are formed (in the sense of a Fermi liquid). The nesting of the two Fermi surfaces gives rise to instabilities of the spin-density and charge-density wave type. For perfect nesting (electron-hole symmetry) an arbitrarily small interaction is sufficient for a ground state with long-range order. The degree of nesting can be controlled by a mismatch parameter, which here was chosen to be the chemical potential, but a magnetic field or disorder in the system have the same effect. In this way the ordering temperature can be tuned to zero, leading to a quantum critical point.

In general there are three independent interaction amplitudes between the electrons and the holes. One corresponds to small momentum transfer, which (without loss of generality) we chose to be isotropic in spin space. The other two interactions represent the momentum transfer **Q** between the pockets with and without spin exchange, respectively. Perturbation theory with respect to these interactions gives rise to dominant logarithmic contributions. We studied the renormalization-group flow of the system in leading and next-to-leading logarithmic order. For repulsive coupling the model renormalizes into the strong-coupling fixed point.

The three interaction amplitudes can in principle cause three types of instabilities, namely charge-density waves (for attractive interaction) and antiferromagnetism parallel and perpendicular to the axis of spin quantization. For $U_{\parallel}=U_{\perp}$ the latter two cannot be distinguished (soft antiferromagnet). Charge-density and spin-density waves exclude each other and can only coexist if in addition there is a ferromagnetic component.[29] We also calculated the linear-response function for the system to antiferromagnetic and charge-density wave order, as well as the precritical fluctuations of the order parameter.

In the disordered phase the heavy fermion system can be described within the Fermi-liquid picture. The effective thermal mass characterizing the low-temperature specific heat is now temperature dependent on a logarithmic scale. The effective mass increases as T is reduced and diverges at the critical point, i.e., T_N. The Néel temperature can be tuned to zero, so that a quantum critical point arises. The divergence of the specific heat γ coefficient signals the breakdown of the Fermi-liquid theory. Similarly the susceptibility to a uniform magnetic field has the usual form expected from Landau's Fermi-liquid theory. The susceptibility is renormalized by two factors: (i) the effective mass, and (ii) a factor that is determined by the interaction vertex between the particles in the two pockets. Both factors diverge at the critical point. In the case of a quantum critical point this divergence occurs at $T=0$. The dependence of χ_B on T at low temperatures is decreasing on a logarithmic scale.

We used a perturbative renormalization approach, which is limited to the weak-coupling region. As the coupling constants are renormalized to larger values, loops to all orders would have to be considered in the renormalization-group equation. The present approach is then unable to describe the critical regime, in which we expect power laws rather than dependences on a logarithmic scale. There is a crossover regime between the weak-coupling and strong-coupling (properties of the fixed point) regimes. This may explain why in some experiments a power law (critical regime), while in others a logarithmic dependence (precritical regime), is observed.

As the critical point is approached, collective modes (spin waves) are formed. These spin waves (bosonic degrees of freedom) are not adequately treated within a perturbative renormalization-group approach. In the weak- and intermediate-coupling regime the collective modes have a broad linewidth and are not relevant. This is, however, not the case in the critical region, where the spin waves are well-defined and play the crucial role. For the critical regime the Hertz-Millis approach,[11,22] which integrates out the fermionic degrees of freedom and obtains an effective bosonic action, is more adequate. Within our approach this would correspond to a finite coupling fixed point, which then yields power-law dependences. We also would like to emphasize that the present approach (although there are some formal analogies) yields results that are physically very different from those of the Kondo problem and Luttinger liquids. This is the consequence of the three dimensionality of the model.

Of great interest is also the low temperature and frequency dependence of the electrical resistivity. The resistivity, however, strongly depends on the disorder in the system and will be discussed in a forthcoming paper.

ACKNOWLEDGMENTS

Support by the Department of Energy under Grant No. DE-FG02-98ER45707 and the National Science Foundation under Grant No. DMR98-01751 is acknowledged.

[1] H. von Löhneysen, Physica B **206&107**, 101 (1994).
[2] M. B. Maple, C. L. Seaman, D. A. Gajewski, Y. Dalichaouch, V. B. Barbetta, M. C. de Andrade, H. A. Mook, H. G. Lukefahr, O. O. Bernal, and D. E. MacLaughlin, J. Low Temp. Phys. **95**, 225 (1994).
[3] C. L. Seaman, M. B. Maple, B. W. Lee, S. Ghamaty, M. S. Torikachvili, J.-S. Kang, L.-Z. Liu, J. Allen, and D. L. Cox, Phys. Rev. Lett. **67**, 2882 (1991).
[4] B. Andraka and A. M. Tsvelik, Phys. Rev. Lett. **67**, 2886 (1991).
[5] B. Andraka and G. R. Stewart, Phys. Rev. B **47**, 3208 (1994).
[6] M. C. Aronson, R. Osborn, R. A. Robinson, J. W. Lynn, R. Chau, C. L. Seaman, and M. B. Maple, Phys. Rev. Lett. **75**, 725 (1995).
[7] O. O. Bernal, D. E. MacLaughlin, H. G. Lukefahr, and B. Andraka, Phys. Rev. Lett. **75**, 2023 (1995).
[8] H. von Löhneysen, T. Pietrus, G. Portisch, H. G. Schlager, A. Schröder, M. Sieck, and T. Trappmann, Phys. Rev. Lett. **72**, 3262 (1994).
[9] A. Rosch, A. Schröder, O. Stockert, and H. von Löhneysen, Phys. Rev. Lett. **79**, 159 (1997).
[10] A. M. Tsvelik and M. Reizer, Phys. Rev. B **48**, 4887 (1993).
[11] A. J. Millis, Phys. Rev. B **48**, 7183 (1993).
[12] M. A. Continentino, Phys. Rev. B **47**, 11 587 (1993).
[13] T. Moriya and T. Takimoto, J. Phys. Soc. Jpn. **64**, 960 (1995); T. Takimoto and T. Moriya, Solid State Commun. **99**, 457 (1996).
[14] E. Miranda, V. Dobrosavljevic, and G. Kotliar, Phys. Rev. Lett. **78**, 290 (1997); Physica B **230-232**, 569 (1997).
[15] D. L. Cox, Phys. Rev. Lett. **59**, 1240 (1987); T.-S. Kim and D. L. Cox, *ibid.* **75**, 1622 (1996).
[16] P. Noziéres and A. Blandin, J. Phys. (Paris) **41**, 193 (1980).
[17] P. B. Wiegmann and A. M. Tsvelick, Pis'ma Zh. Éksp. Teor. Fiz. **38**, 489 (1983) [JETP Lett. **38**, 591 (1983)]; A. M. Tsvelick and P. B. Wiegmann, Z. Phys. B **54**, 201 (1984); N. Andrei and C. Destri, Phys. Rev. Lett. **52**, 364 (1984).
[18] P. Schlottmann and P. D. Sacramento, Adv. Phys. **42**, 641 (1993).
[19] M. Jarrell, H. Pang, and D. L. Cox, Phys. Rev. Lett. **78**, 1996 (1997); F. B. Anders, M. Jarrell, and D. L. Cox, *ibid.* **78**, 2000 (1997).
[20] The entire Brillouin zone can participate in the nesting for a lattice consisting of two interpenetrated sublattices, like a sc or bcc lattice. In this case **Q** is commensurate with the lattice.
[21] D. R. Penn, Phys. Rev. **142**, 350 (1966); S. K. Chan and V. Heine, J. Phys. F **3**, 795 (1973).
[22] J. A. Hertz, Phys. Rev. B **14**, 1165 (1976).
[23] V. N. Popov, *Functional Integrals in Quantum Field Theory and Statistical Physics* (Kluwer Academic, Hingham, MA, 1983).
[24] R. Shankar, Rev. Mod. Phys. **66**, 129 (1994).
[25] A. C. Hewson, Adv. Phys. **43**, 543 (1994).
[26] H. J. Schulz, Europhys. Lett. **4**, 608 (1987).
[27] N. Menyhárd and J. Sólyom, J. Low Temp. Phys. **12**, 529 (1973).
[28] J. Sólyom, Adv. Phys. **28**, 201 (1979).
[29] C. A. Balseiro, P. Schlottmann, and F. Yndurain, Phys. Rev. B **21**, 5267 (1980).
[30] A. A. Abrikosov and A. A. Migdal, J. Low Temp. Phys. **3**, 519 (1970); M. Fowler and A. Zawadowski, Solid State Commun. **9**, 471 (1971).
[31] J. Sólyom, J. Low Temp. Phys. **12**, 547 (1973).
[32] J. M. Luttinger, Phys. Rev. **119**, 1153 (1960).
[33] A. A. Abrikosov, L. P. Gor'kov, and I. E. Dzyaloshinski, *Methods of Quantum Field Theory in Statistical Physics* (Dover Publications, New York, 1963).
[34] A. Yoshimori, Prog. Theor. Phys. **55**, 67 (1976); H. Shiba, *ibid.* **54**, 967 (1975); L. Mihály and A. Zawadowski, J. Phys. (France) Lett. **39**, L483 (1978); P. Schlottmann, Phys. Rev. B **21**, 1084 (1980).
[35] P. Nozières, *Theory of Interacting Fermi Systems* (Addison-Wesley, Reading, 1964), Chap. 6.
[36] Yu. A. Bychkov, L. P. Gor'kov, and I. E. Dzyaloshinski, Zh. Éksp. Teor. Fiz. **50**, 738 (1966) [Sov. Phys. JETP **23**, 489 (1966)].
[37] K. Yosida, Phys. Rev. **147**, 223 (1966); Prog. Theor. Phys. **36**, 875 (1966).